ELSEVIER

Polymer 43 (2002) 3999–4010

polymer

www.elsevier.com/locate/polymer

Evaluation of the instantaneous nucleation density in the isothermal crystallization of polymers

J.A. Martins[a,*], J.J.C. Cruz Pinto[b]

[a]*Departamento de Engenharia de Polímeros, Universidade do Minho, Campus de Azurém, 4800-058 Guimarães, Portugal*
[b]*Departamento de Química, Universidade de Aveiro, 3810-193 Aveiro, Portugal*

Received 4 May 2001; received in revised form 22 March 2002; accepted 26 March 2002

Abstract

An expression is established for the temperature dependence of the average density of nuclei, as well as a temperature-dependent relationship between the half-crystallization times, $t_{50\%}$, obtained from isothermal differential scanning calorimetry polymer crystallization experiments, and the linear spherulite growth rate, G, obtained by hot-stage optical microscopy. This relationship allows the evaluation of the mean number of nuclei per unit volume grown at a given crystallization temperature. For an athermal nucleation, the spatial density of nuclei is simply related to their surface density in a sample's cross-section, and the experimentally observed mean number of nuclei is compared with the predicted value, at each crystallization temperature. It is also shown that the ratio between the temperature dependencies of $\ln(1/t_{50\%})$ and $\ln(G)$ may be used as an indicator of the nucleation type and of the morphology developed.

Keywords: Isothermal crystallization; Spherulite; Nuclei

1. Introduction

Differential scanning calorimetry (DSC) and polarized light optical microscopy are widely used in studies on polymer crystallization kinetics. However, to our knowledge, an uncontroversial relationship between the results obtained by these techniques has not yet been obtained. The establishment of such a relation would highlight the applicability range of each technique and allow the mutual validation of the resulting data.

Some authors have been using indistinctively data obtained with both these techniques to get information on the lamellae folding and lateral surface energies. The only reliable quantitative information concerning those energies is that obtained from optical microscopy data. The values of the surface energies obtained from DSC half-crystallization time data, with no additional data treatment procedures, may exceed by more than 20% the values directly obtained from optical microscopy measurements [1–3]. These deviations have so far been considered acceptable within the experimental errors, particularly given the complexity of the overall crystallization kinetics. In fact, provided that the experiments are carefully planned, the above difference turns out to have a physical meaning, allowing the evaluation of the *temperature dependence of the nucleation density*.

The evaluation of this temperature dependence is done in this work, following standard procedures [4,5], and it allows the establishment of a relationship between the data obtained by optical microscopy and DSC, which is not straightforward. Some assumptions must be made that restrict its applicability.

The quiescent crystallization of many common industrial polymers may, as a first approximation, be considered the result of a mainly athermal nucleation. Neglecting the columnar structures (or upper and lower transcrystalline layers), the equiaxed spherulites may be visualized as a packing of convex polyhedrons. The classical theories for the overall crystallization kinetics may then be used to predict the nucleation and growth parameters of these three-dimensional structures. It is well known, from studies on polymer global crystallization kinetics, that Avrami exponents provide information on the dimensionality of the growing structures and on its type of nucleation. The non-integer nature of these exponents is generally attributed to the competition of a diffusion-controlled growth and/or to the irregular boundary of the spherulites [6,7].

* Corresponding author. Tel.: +351-2535-10245; fax: +351-2535-10249.

E-mail addresses: jamartins@dep.uminho.pt (J.A. Martins), cpinto@dq.ua.pt (J.J.C. Cruz Pinto).

0032-3861/02/$ - see front matter
PII: S0032-3861(02)00221-5

In a first stage, only the isothermal crystallization with instantaneous (or athermal) nucleation will be analysed. This type of nucleation was selected because it makes easier to obtain an expression for the temperature dependence of the mean number of nuclei per unit of volume. Of course, a truly instantaneous activation of nuclei is a theoretical idealization. In practice, a nucleation activation process may be considered instantaneous when the rate of activation of nuclei is much larger than its growth rate. In some practical situations, where the nucleation is of the mixed type, the prediction of the density of nuclei as a function of temperature is much more difficult and still challenging task.

For the specific case under study, this prediction may be experimentally verified through the analysis of sections of samples isothermally crystallized in a DSC. Provided that the nucleation is athermal, and the distribution of nuclei is Poissonian, a direct relationship is known to exist between the mean number of nuclei per unit volume and per unit surface [8–10]. Van de Weygaert discussed the validity of the above relationship [11]. Further assumptions on this analysis may allow us to estimate the average diameter of the equiaxed spherulites (which may also be checked against experiments). This prediction is of the utmost importance, because of the role played by the morphology, namely the spherulite size, on the mechanical properties [12,13].

2. Theory

2.1. Single mechanism equations

It is not the purpose of this work to discuss the theoretical background and limitations of the equations generally used in the description of the overall crystallization kinetics, which is usually described by single mechanism equations, such as Avrami/Evans equation [14,15]. A more general reasoning, used by Kolmogoroff [16], allows the derivation of an equation that reduces to Avrami equation under the assumption of constant growth rate of solid structures and a nucleation rate equal to $(N_V/\tau)\exp(-t/\tau)$, where N_V is the average number of potential nuclei per unit volume and τ is the activation time. The assumptions under the derivation of Kolmogoroff equation are of a geometrical nature and include the validity of a Poissonian distribution of nuclei. The general form of Avrami equation is

$$X(t) = 1 - \exp(-kt^n), \tag{1}$$

where k and n have their usual meanings. Assuming the non-diffusion-controlled growth of perfect spheres, n should be 3 for athermal nucleation, and 4 for thermal nucleation. Another equation, with the same starting point as Avrami equation, but with a different way of accounting for the impingement between solid growing structures is Tobin equation [17],

$$\frac{X(t)}{[1 - X(t)]} = kt^n. \tag{2}$$

Limitations concerning the application of Avrami equation have been discussed [18–20]. Among these limitations is a constant growth rate of the solid structures, an assumption that was verified experimentally by the measurement of the spherulite growth rate at constant temperature for the samples studied in this work. Those measurements were performed up to and after the occurrence of the impingement between the growing structures, with the same results.

The temperature dependence of the linear growth rate of the spherulites may be derived from the Lauritzen–Hoffman theory for secondary nucleation [21]. Assuming a coherent secondary surface nucleation, the linear growth rate is

$$G(T) = G_0 \exp\left(-\frac{\Delta G_d}{k_B T}\right)\exp\left(-\frac{K_g}{T\Delta T f}\right), \tag{3}$$

where ΔG_d is the activation energy for the transport of a supercooled stem to the semicrystalline nuclei, T the absolute temperature, K_g a parameter related to the fold and lateral surface energies, ΔT the supercooling (difference between the thermodynamic melting temperature, T_m^0, and the crystallization temperature) and f a corrective factor for the decrease of the enthalpy of fusion with the crystallization temperature. A general formula for K_g is $K_g = cb_0\sigma\sigma_e T_m^0/(k_B \Delta H_f^0)$, where c is 4 for regimes I and III and 2 for regime II, the other parameters having their usual meanings [21].

2.2. Calculation of half-crystallization times

From isothermal crystallization experimental data, as obtained in a DSC, the time corresponding to half of the overall phase change, $t_{50\%}$, is related to the kinetic constants of Eqs. (1) and (2) by

$$t_{50\%} = \left(\frac{A}{k}\right)^{1/n}, \tag{4}$$

with $A = \ln 2$ for Eq. (1) and $A = 1$ for Eq. (2), which may be expressed as a function of the spherulite growth rate as

$$\frac{1}{t_{50\%}} = (C_A \bar{N})^{1/n} G, \tag{5}$$

with $n = 3$ and $C_A = 4\pi\rho_s/(3\rho_l \ln 2)$, with C_A replaced by $C_T = 4\pi\rho_s/3\rho_l$ for Tobin's approach. $\bar{N}$ is the average number of nuclei per unit volume of untransformed material. For sporadic nucleation, the corresponding relationship is

$$\frac{1}{t_{50\%}} = \left(\frac{C_A \dot{N}}{4}\right)^{1/n} G^{(n-1)/n}, \tag{6}$$

with $n = 4$, where $\dot{N}$ is the nucleation rate. A similar expression may be obtained for Tobin equation, with C_A replaced by C_T.

For an athermal (instantaneous) nucleation of spheres, it is generally assumed that the temperature dependence of the reciprocal of the half-crystallization time is the same as the linear growth rate, in Eq. (3)

$$\frac{1}{t_{50\%}} = (C\bar{N})^{1/3} G_0 \exp\left(-\frac{\Delta G_d}{k_B T}\right)\exp\left(-\frac{K_g}{T\Delta Tf}\right), \tag{7}$$

with $C = C_A$ or $C = C_T$, depending on the formalism used. The validity and consequences of this usual assumption should now be examined.

In these conditions, a plot of $\ln(1/t_{50\%})$ versus $(1/T\Delta Tf)$ should be vertically shifted from a plot of $\ln(G)$ versus $(1/T\Delta Tf)$ by $(1/3)\ln(C\bar{N})$. According to the definition of an instantaneous nucleation [18], and assuming that the average number of potential nuclei in the melt is constant, all the nuclei should be activated at the start of the crystallization and, therefore, $\bar{N}$ should be constant for all crystallization temperatures. This would imply that the vertical shift between the experimental results of the linear growth rate, obtained by hot-stage polarized optical microscopy, and the results of the half-crystallization time, obtained by DSC, should be constant for all crystallization temperatures.

In practice, however, it is found that this vertical shift increases when the crystallization temperature decreases, which is consistent with an increase of the real number of activated nuclei with decreasing crystallization temperatures, which, for a particular crystallization temperature, is

$$\bar{N} = \frac{1}{C}\exp\left[3\ln\left(\frac{1/t_{50\%}}{G}\right)\right]. \tag{8}$$

It must be stressed that the possible temperature dependence of the average number of nuclei is not made explicit in Eq. (5) or (7) although it is automatically accounted for in the value of the reciprocal half-crystallization time experimentally recorded for each crystallization temperature.

Although, from a strict physical point of view, one would expect the same K_g values from Eqs. (3) and (7), it is experimentally found that they are different. It is now in order to make explicit the temperature dependence of $\bar{N}$ and to analyse its effect on the *apparent* K_g value measured from the $(1/t_{50\%})$'s variation with temperature.

Before proceeding with the analysis, it must be remembered that $\bar{N}$, in all the above equations, is the average number of nuclei per unit volume of *untransformed* material. The conversion to average number of nuclei per unit volume of *transformed* material ($\bar{N}_t$) is $\bar{N}_t = \bar{N}(\rho_s/\rho_l)$. In what follows, only $\bar{N}_t$ will be used, the above conversion being implicit in the new constants $C_{A,t} = (\rho_l C_A)/\rho_s$ and $C_{T,t} = (\rho_l C_T)/\rho_s$.

2.3. Temperature dependence of the average density of nuclei, $\bar{N}_t$

A procedure used to evaluate the average density of nuclei was first proposed by Kurz and Fisher [4], and is also implicitly assumed in textbooks on solidification of metals and alloys [22]. The entropy of mixing between embryos and atoms is evaluated by assuming that they have the same size. After evaluating the free energy difference between two systems, one with a mixture of embryos and atoms (segments, in the present case) and another containing only atoms/segments, the number of embryos at equilibrium is evaluated. Although the procedure followed by Kurz is inaccurate, since the embryos are much larger than the atoms/segments, it will be assumed in this work that the temperature dependence of the average density of nuclei is that obtained from the Kurz and Fisher procedure and that it is valid, at least as an approximation. The result obtained from this approach for the number of embryos with critical size, N_e^*, at equilibrium with segments is

$$N_e^* \cong N_s \exp\left[-\frac{\Delta G_e^*}{k_B T}\right], \tag{9}$$

where ΔG_e^* is the free energy of activation for the formation of one critical embryo and N_s is the total number of chain segments in the mixture. We assume that a more accurate evaluation would maintain the Boltzmann factor unchanged and that the only changes, as a result of the embryos and segments having different sizes, would be reflected upon the pre-exponential factor.

The reasons for adopting the above expression are discussed in Appendix A, the main one being that an accurate evaluation of the number of possible combinations of objects with different sizes has not previously been made. A possible procedure to be followed in such evaluation is also presented in Appendix A.

The main assumption that led to Eq. (9) is an ideal equilibrated solution (at a given temperature T) between segments and embryos, whose validity is restricted to ideally pure and equilibrated substances. This equilibrium (or pseudo-equilibrium) assumption is indeed as doubtful, or as reasonable, as the one made within the theory of absolute reaction rates, where an equilibrium is also assumed between the system's activated complex and the reactant molecules involved. All that in fact needs to be assumed is an extremum (maximum) of the Gibbs free energy (which indeed it must always be, as imposed by the nucleation theories), and it is also perfectly reasonable to expect (exactly as in any real, actually occurring, chemical reaction or other physical process) that such extremum is the minimum (for the most probable, and fastest, transformation path) of all possibly existing maxima of the (configurational) Gibbs free energy. All alternative configurations would lead to (much) lower transformation rates.

The critical free energy of activation for heterogeneous nucleation of a rectangular nucleus with base (ab) and thickness (l) in a plane substrate is

$$\Delta G_e^* = \frac{16\Delta\sigma\sigma\sigma_e\left(T_m^0\right)^2}{(\Delta h_f \Delta T)^2}, \tag{10}$$

where $\Delta\sigma$ is the specific interfacial surface free energy, due to one surface being in contact with the polymer melt and another with the heterogeneous nucleus [18].

For high supercooling, the thickness of the nucleus is the same as that of a chain stem, $b^* = b_0$, the area of the base being now ab_0. Assuming, in addition, that $\Delta\sigma$ is small (virtually zero), a condition that may be matched when the substrate has the same nature as the nuclei, or when the crystallographic orientation of the chains in the nucleus is the same as that of the molecules in the heterogeneous substrate (case of epitaxy), the critical free energy for heterogeneous nucleation of a rectangular nucleus with base (ab_0) and thickness (l) in a plane substrate is

$$\Delta G_e^* = \frac{4b_0\sigma\sigma_e T_m^0}{\Delta h_f \Delta T}. \tag{11}$$

The substitution of Eq. (11) into Eq. (9) leads to

$$N_e^* \cong N_s \exp\left(-\frac{K_n}{T\Delta T}\right), \tag{12}$$

with $K_n = 4b_0\sigma\sigma_e T_m^0/(k_B\Delta H_f^0)$, which has the same temperature dependence of the spherulite growth rate, Eq. (3).

Assuming now that the average number of critical embryos per unit volume is the same as the average number of nuclei, $\bar{N}$ (or $\bar{N}_t$), the substitution of Eq. (12) into Eq. (7) allows the definition of an apparent value for $K_g^{1/t_{50\%}} = (K_n/3) + K_g$. This then explains why the slope of $\ln(1/t_{50\%})$ versus $(l/T\Delta Tf)$ is higher, $K_g^{1/t_{50\%}} > K_g^G$, where $K_g^G = K_g$ is the slope of $\ln(G)$ versus $[1/(T\Delta Tf)]$.

The pre-exponential factor in Eq. (7), resulting from the substitution of Eq. (12), is proportional to $(N_s)^{1/3}$. The number of atoms (or chain segments) to be added to an embryo should, of course, be temperature and material dependent. The material dependence may be established from the sequences of *trans–gauche* conformations of a chain stem within the amorphous phase (supercooled melt). The temperature dependence should be proportional to $\{1 + 2\exp[-\Delta E/(k_B T)]\}^{-1/3}$, where ΔE is the energy difference between *gauche* and *trans* states. Since, as a simplification, we are interested in a temperature dependence proportional to $\exp(-1/T\Delta T)$, we will neglect at this stage the temperature dependence of N_s (of the above Boltzmann's type), which is clearly much less significant than that of the latter exponential factor. In any case, what is evaluated is $\bar{N}$ (or $\bar{N}_t$), and not N_s.

If one now assumes that the surface energies involved in the formation of the primary nuclei are the same as those involved in the formation of the secondary nuclei (during growth), then $K_n = K_g^G$, and the apparent value of $K_g^{1/t_{50\%}}$ for an instantaneous nucleation of spheres is $(4/3)K_g^G = 1.333K_g^G$. Similarly, for an instantaneous nucleation of disks and rods, the relationship is $K_g^{1/t_{50\%}} = (3/2)K_g^G$ and $K_g^{1/t_{50\%}} = 2K_g^G$, respectively.

Differences in the exact nature of the above nucleation and growth processes may result in (possibly small) deviations in the previously mentioned numerical factor. The ratio between $K_g^{1/t_{50\%}}$ and K_g^G may also be a useful parameter to evaluate to what extent the solidification of a material may be described by an instantaneous nucleation process and the reasonableness of assuming that the shape of the semicrystalline growing structures is spherical.

2.4. Evaluation of the average density of nuclei

Having established the temperature dependence of the reciprocal of the half-crystallization time, because of the nearly linear dependence on $(1/(T\Delta Tf))$ of the experimental values of both $\ln(1/t_{50\%})$ and $\ln(G)$, the number of activated nuclei per unit volume, at each crystallization temperature, may then be estimated from Eq. (8). The result is

$$\ln(C_{A,t}\bar{N}_t) = 3\left(K_g^G - K_g^{1/t_{50\%}}\right)\frac{1}{T\Delta Tf} + 3\left[\ln\left(\frac{1}{t_{50\%}}\right)_0 - \ln(G)_0\right], \tag{13}$$

where, as previously stated, instantaneous nucleation is assumed. The density of nuclei may thus be evaluated by Eq. (8) or (13) using only experimental data obtained from two of the most widely used techniques in polymer crystallization kinetic studies. Eq. (8) is used only when the experimental data of G and $t_{50\%}$ are available for the same crystallization temperatures. Often, however, the experimental data obtained with one of the techniques need to be extrapolated to another temperature range and Eq. (13) should then be used to evaluate the average density of nuclei. The assumption of constant $K_g^{1/t_{50\%}}$ and K_g^G is valid only under conditions of constant growth regime.

The density of nuclei may also be evaluated from values of the kinetic constants of Avrami's and Tobin's equations, found from the best fit of these equations to the experimental data. Using a procedure similar to that used in the derivation of Eq. (13), we may define a K_g^k ($>K_g^G$) as the slope of a line in a graph of $\ln(k^{1/n})$ versus $1/T\Delta Tf$, which already accounts for the temperature dependence of the average density of nuclei according to Eq. (12). The average density of nuclei is

$$\ln(C\bar{N}_t) = 3\left(K_g^G - K_g^k\right)\frac{1}{T\Delta Tf} + 3[\ln(k)_0 - \ln(G)_0], \tag{14}$$

with $n = 3$ and $C = 4\pi/3$. The formal relationship is independent of the model chosen but the values of K_g^k and $\ln(k)_0$ are model-dependent.

In Eqs. (13) and (14), $\ln(1/t_{50\%})_0$, $\ln(G)_0$ and $\ln(k)_0$, which are the intercepts at the origin, are evaluated, respectively, from plots of $\ln(1/t_{50\%})$, $\ln(G)$ and $\ln(k)$ plus the transport term against $[1/(T\Delta Tf)]$. The transport term in Eq. (3) is usually assumed to have WLF functionality, i.e. $\Delta G_d/k_B T = C_1C_2/(C_2 + T - T_g)$, with C_1 and C_2 having approximately constant values of 25 and 30 K, respectively, as a result of

adopting the polymer's specific T_g value as the reference temperature.

2.5. Relationship between the volume and surface densities of nuclei

A three-dimensional picture of a Poissonian distribution of $\bar{N}_t$ nuclei, formed instantaneously, may be obtained from a Monte-Carlo simulation. The smallest volume cell surrounding each nucleus is the Wigner–Seitz cell [23]. The $\bar{N}_t$ cells are known as the elements of a Voronoi tessellation, Wigner–Seitz cells, Dirichlet regions or Thiessen figures. A generalization of the Voronoi tessellation is the Johnson and Mehl model, which contains a dynamic element: the growth of each nucleus with a linear and isotropic velocity [24]. It was shown that, if all nuclei are generated at the same instant, the resulting tessellation is of the Voronoi type [11].

Statistical moments of three-dimensional Voronoy tessellations were determined numerically by Gilbert [8] and analytically by Miles and Møller [9,10], who also established expressions for the lower dimensional sections, line and plane sections through two- and three-dimensional tessellations, respectively. These stereological properties of tessellations are important for the calculation of the volume density of cells from a surface analysis of sections of a sample. A listing of the moments of two-dimensional sections through three-dimensional Poisson–Voronoy tessellations was given by Van de Weygaert [11]. For the case of interest, the relationship is

$$\bar{\sigma} = \frac{\Gamma(1/3)\left(16\pi^5 \bar{N}_t^2/9\right)^{1/3}}{15} = 1.4580\bar{N}_t^{2/3}, \tag{15}$$

where $\bar{\sigma}$ is the surface density of nuclei and Γ is the gamma function. Other relationships exist between the area and perimeter of the cell and the number of nuclei per unit volume.

A final relationship between the volume density of nuclei and its average diameter is more difficult to establish, mainly because it is impossible to fill 100% of the volume with spheres. Additional hypothesis concerning the final shape of the spherulites must be made, namely, the definition of a convex polygon involving the spherulite, the fraction of volume occupied by an arrangement of such polygons and the evaluation of their equivalent diameter.

Other known works in the area of crystallization kinetics are, among others, those of Eder et al. [19] and Isayev and Cagtinani [25]. From the definition of the kinetic constant, k, and assuming that the potential nucleation sites have already a spherical shape, it is possible to derive an expression for the average distance between the nuclei [23,26]. It may also be found in the literature an equation similar in role to Eq. (14),

$$\bar{N}(T) = \frac{3V_\infty}{4\pi}\left[\frac{Z(T)}{G(T)}\right]^n, \tag{16}$$

where V_∞ is the maximum volume fraction of spherulites at infinite time, where $Z(T)$ $(= k(T)^{1/n})$ is the kinetic constant of Nakamura/Avrami equation for non-isothermal crystallization. Isayev and Cagtinani used it to predict the density of nuclei and the average spherulite size in injection moulded samples [25].

We do not know of any application made by Eder et al. of Eq. (16) to predict the average density of nuclei. They have effectively measured the surface density of nuclei for samples crystallized at selected temperatures [27], and the sample's crystallization temperature was corrected in order to account for its thermal resistance and for the heat released during crystallization. A volume density was then calculated (assuming that $\bar{N}_t \cong (\bar{\sigma})^{3/2}$), which is overestimated by a factor of $1.458^{3/2}$, see Eq. (15). No comparison of this experimental nuclei density was made with the value predicted from Eq. (16).

As for the work of Isayev et al., they calculate, for non-isothermal crystallization experiments, an induction time for each cooling rate, by subtracting the thermodynamic melting temperature to the temperature of the start of the crystallization and by dividing the difference by the cooling rate. Experimental results are corrected for the induction time. An additional data correction is performed to account for the sample's thermal resistance and the release of the heat of crystallization, according to a method proposed by Janeschitz-Kriegl. No reference was made to a calibration on *cooling* of experimental data. The Nakamura equation is then fitted to the data and the parameters of $Z(T)$—a pre-exponential factor and the argument of the exponential related to the secondary nucleation—found from the best fit to the data. The additional procedure to deal with the effect of the processing conditions on the crystallization development may be found in the above reference and in the references therein. Somewhat surprisingly, they apparently succeeded in predicting the final spherulite size as a function of the processing conditions. However, the procedure used by Isayev et al., as acknowledged by the authors, corrects the experimental data for an induction time that depends on the sensitivity of the measuring device and on the quantity being measured. The use of such arbitrarily defined, device-dependent, induction times clearly lacks a physical basis and is therefore difficult to justify.

It has recently been shown that the procedure described here, which uses Eq. (13) to evaluate the average density of nuclei from DSC and optical microscopy data, and Eq. (15) to make the conversion from a surface density to a volume density of nuclei, may be applied to non-isothermal crystallization of polymers under quiescent conditions. It has also been successfully applied to the prediction of the average spherulite size in rotationally moulded parts [28].

3. Experimental

Two semicrystalline polymers have been used in this

work, polyoxymethylene (POM) and a grade of medium density polyethylene (MDPE) appropriate for rotational moulding applications. The POM sample was a Delrin 150, with $\bar{M}_n = 70\,000$ g/mol, $T_m^0 = 188.91$ °C, $T_g = -60.2$ °C and an enthalpy of fusion for a 100% crystalline sample of $\Delta H_f^0 = 326$ J/g [29]. The crystallinity of this sample, evaluated from DSC data, varies from 50% (crystallized at 149 °C) to 54% (crystallized at 157 °C). Values of the crystallinity of POM Derin 150 homopolymer, measured by X-ray diffraction, are much higher ($\approx 75\%$) [30]. The MDPE sample, from Enichem, RP264H, with $\bar{M}_w = 31\,000$ g/mol, $T_m^0 = 143$ °C, $T_g = -80$ °C and enthalpy of fusion for an 100% crystalline sample of $\Delta H_f^0 = 293$ J/g [29] has a crystallinity between 33% (crystallized at 108 °C) and 41% (crystallized at 116 °C). The sample masses of POM and MDPE were, respectively, 4.328 and 10.313 mg. The thermodynamic melting temperatures were measured from Hoffman and Weeks plots. Other values were taken from Ref. [31].

The isothermal crystallization experiments have been performed in a Perkin–Elmer DSC 7, with a constant temperature (5 °C) cell cooling block. Nitrogen was used as purge gas. Hand-crimped aluminium pans have been used for both materials. Prior to the experiments, temperature and heat flow rate calibrations were performed with standard metals at the lowest, fully controllable, scanning rate of the device, 0.1 °C/min. Calibration checks at this same scanning rate have been performed at the start and end of a set of experiments. The temperature deviations between the measured indium onsets were always less than 0.1 °C.

The temperature program was as follows: 5 min at a temperature higher than the thermodynamic melting temperature (T_{start}); 1 additional minute at T_{start} for the definition of a base line at the start of the experiment; temperature program at −80 °C/min to the crystallization temperature. The dwell time at the crystallization temperature was long enough to ensure the complete recording of the crystallization process, and it was measured since the attainment of the selected isothermal crystallization temperature, with no allowance for any induction time. For each crystallization temperature, a blank run was also carried out. Although the above procedure is almost standard practice in isothermal crystallization experiments, it is important for a correct definition of the base line at the start of the isothermal and for a more precise determination of the time corresponding to 50% of crystallization.

The measurements of the linear growth rate of the spherulites have been performed in a Mettler hot-stage coupled to a polarized light optical microscope. Prior to the experiments, and in order to quantify eventual errors, a calibration check of the hot-stage measured temperature was performed. The clearing temperature of phenacetin was recorded at a scanning rate of 0.1 °C/min and compared with the onset temperature of the melting transition measured in a calibrated DSC at the same rate. Differences in temperature of less than 1 °C have been obtained.

To evaluate the number of spherulites crystallized in the DSC at different temperatures, several sections were cut from the corresponding crystallized samples, which were then analysed. The borders of the spherulites were outlined and an average number per unit section area was measured for the equiaxial spherulites. Due to their reduced dimension, the columnar spherulites, on the top and bottom surfaces, were neglected.

4. Results

4.1. Crystallization kinetics

Although the description of the crystallization kinetics is not the main topic of this work, as a discussion on the crystallization kinetics of these materials was reported elsewhere [20,32], only the predictions supplied by both model equations (1) and (2) are compared. The purpose is to make use of the best values for the kinetic constants to predict the average density of nuclei from Eq. (14) (similar to the procedure used by Isayev and Cagtinani in their work [25]) and to compare the predicted values for n with the ratio $K_g^{1/t_{50\%}}/K_g^G$.

The results obtained for the description of the experimental data with Avrami and Tobin equations are shown in Fig. 1, for POM, and in Fig. 2, for MDPE. In both figures, full lines stand for Tobin's equation (Eq. (2)), while dashed lines stand for Avrami's equation (Eq. (1)). Values of the parameters for both materials obtained with these equations are shown in Tables 1 and 2, for POM and MDPE, respectively.

Since the procedure, described earlier, to calculate the average number of nuclei assumes an athermal nucleation, the description of the isothermal crystallization with a constant n (=3) was performed and the best value of the

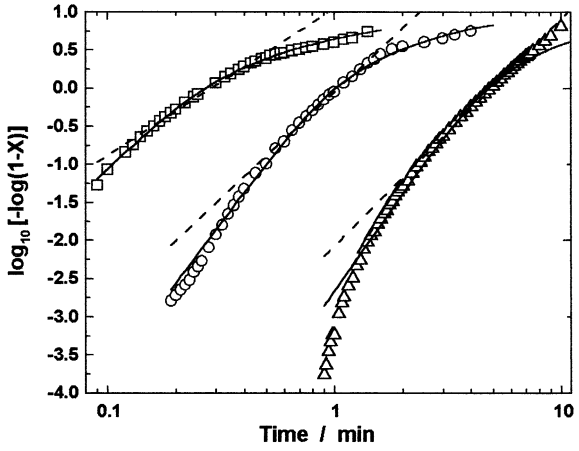

Fig. 1. Isothermal crystallization of POM at (□) 149 °C, (○) 153 °C and (△) 157 °C. Dashed line is the fit obtained with Avrami equation; solid line is the fit obtained with Tobin equation. Sample mass = 4.328 mg.

Table 1
Values of Avrami and Tobin parameters for the isothermal crystallization of POM at the indicated temperatures. For both models, the values of the kinetic constant, for a constant $n = 3$, are also shown

T (°C)	Avrami			Tobin		
	K ($\times 10^4$ min^{-n})	n	K ($n = 3$) ($\times 10^6$ min^{-3})	K ($\times 10^6$ min^{-n})	n	K ($n = 3$) ($\times 10^6$ min^{-3})
149	2440	1.93	245.79	27 200	2.94	398.18
150	775	2.20	132.03	5540	3.30	215.83
151	192	2.44	54.43	1110	3.50	91.95
152	49.2	2.58	19.01	169	3.68	30.17
153	5.93	2.78	4.19	9.02	3.95	6.65
154	0.568	3.03	1.09	0.432	4.24	1.72
155	0.196	3.04	0.40	0.0934	4.27	0.62
156	0.0638	3.06	0.14	0.0155	4.34	0.23
157	0.0249	2.98	0.039	0.00339	4.26	0.064

Table 2
Values of Avrami and Tobin parameters for the isothermal crystallization of MDPE. For both models, the values of the kinetic constant, for a constant $n = 3$, are also shown

T (°C)	Avrami			Tobin		
	K ($\times 10^6$ min^{-n})	n	K ($n = 3$) ($\times 10^6$ min^{-3})	K ($\times 10^6$ min^{-n})	n	K ($n = 3$) ($\times 10^6$ min^{-3})
107	1120	3.21	37.57	1640	4.64	59.80
109	267	3.36	16.03	2.42	4.81	25.05
111	66	3.39	5.12	0.271	4.91	8.39
113	14.4	3.30	0.93	0.0634	4.61	1.45
115	12.2	2.83	0.078	0.0216	4.11	0.13
117	6.6	2.47	0.0035	0.00518	3.67	0.0062

only changing parameter—the kinetic constant—estimated for each crystallization temperature. This value is also shown in Tables 1 and 2 for both materials and model equations.

For POM, irrespective of equation (1) or (2) used and of the value of n (constant = 3 or variable), the sum of least squared differences (SLS) had approximately the same value ($\sim 10^{-2}$), which may confirmed by the results of Fig. 3, where $\ln(k^{1/n})$ is plotted against $1/T\Delta Tf$. The analysis

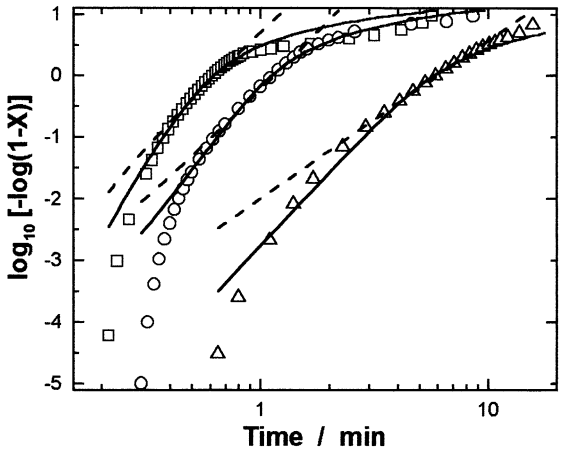

Fig. 2. Isothermal crystallization of MDPE at (□) 115 °C, (○) 121 °C and (△) 125 °C. Dashed line is the fit obtained with Avrami equation; solid line is the fit obtained with Tobin's equation. Sample mass = 10.313 mg.

of the morphology of the samples, crystallized at these same temperatures, confirm that the nucleation is mostly sporadic for temperature between 154 and 157 °C [20], according to the prediction supplied by Tobin's equation.

For MDPE, the SLS also had approximately the same value ($\sim 10^{-2}$) for Eq. (1) and n constant = 3 or variable. Slightly lower values of the SLS are obtained with Tobin equation with n variable, but microscopic observations of the microtomed samples' sections shows that the nucleation is athermal with fully developed spherulites [32]. Also, for MDPE, the temperature dependence of $\ln(1/t_{50\%})$, obtained from the DSC results, and the kinetic constants of Avrami and Tobin equations (with n variable and equal to 3) is the same as that of the growth rate, as it may be checked by plotting those results as a function of $1/(T\Delta Tf)$ in Fig. 4. In Figs. 3 and 4, the results of $\ln(k^{1/3})$ are represented by the dotted lines, which are almost undistinguishable from those $\ln(k^{1/n})$ with variable n.

4.2. Comparison between $(1/t_{50\%})$ and G

Figs. 5 and 6 compare the results of $\ln(1/t_{50\%})$ and $\ln(G)$. The shift factor between them is proportional to, and thus enables to evaluate, the density of nuclei. The ratio $K_g^{1/t_{50\%}}/K_g^G$ is 1.124 for POM and 1.283 for MDPE. We remember that, for an instantaneous nucleation of perfect spheres, this ratio should be 1.333. The isothermal crystallization of MDPE may then be approximately described by

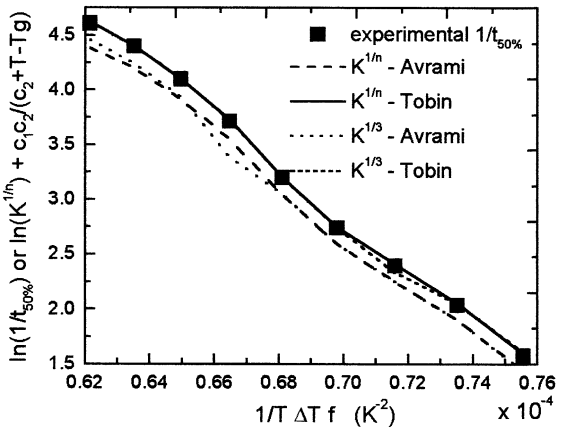

Fig. 3. Values of the logarithm of the reciprocal of the half-crystallization time, obtained from DSC measurements for the isothermal crystallization of POM, and values of $\ln(k)^{1/n}$ and $\ln(k)^{1/3}$, obtained from the fits to the experimental data with Avrami and Tobin equations. The results are plotted against $1/(T\Delta Tf)$. Time is in minutes.

an instantaneous nucleation of spherulitic structures, seemingly according to the description supplied by Avrami equation. For POM, the nucleation is sporadic and the crystallization process seems to be better described by Tobin equation.

For some crystallization temperatures, the density of nuclei was also experimentally evaluated by sectioning the samples crystallized at the selected temperatures, and by counting the number of spherulites in each photograph per unit viewed section area. In doing so, the upper and lower transcrystalline layers were neglected, as well as the columnar spherulites that appear in some of the MDPE samples. Due to the reduced volume of these structures, compared to the total volume of the samples under analysis, it is assumed that their contribution to the total density of nuclei may be neglected.

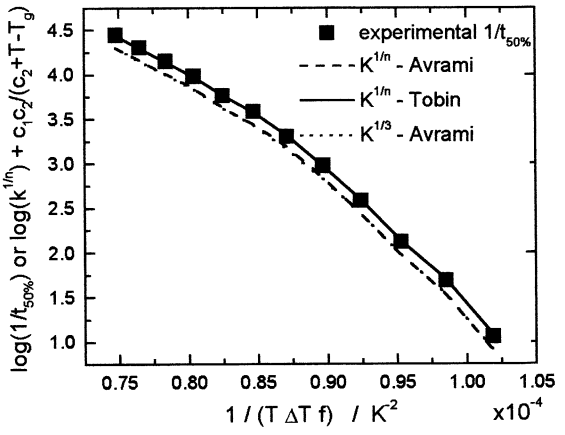

Fig. 4. Values of the logarithm of the reciprocal of the half-crystallization time, obtained from DSC measurements for the isothermal crystallization of MDPE, and values of $\ln(k)^{1/n}$, obtained from the fits to the experimental data with Avrami and Tobin equations. For $\ln(k)^{1/3}$, only the results obtained with Avrami's equation are shown. The results are plotted against $1/(T\Delta Tf)$. Time is in minutes.

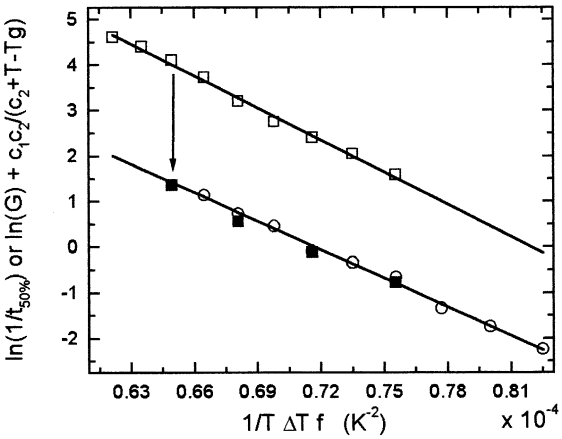

Fig. 5. Comparison of values of the logarithm of the reciprocal of the half-crystallization time (□) with values of the logarithm of the growth rate (○) for the isothermal crystallization of POM. The half-crystallization time plot, when subtracted of the contribution of the mean number of nuclei (first factor on the right-hand side of Eq. (7)) is shifted and becomes coincident with the growth rate plot (■). The experimental densities of nuclei are for 151, 153, 155 and 157 °C. Time is in minutes and G in mm/min.

When the results of $\ln(1/t_{50\%})$ are subtracted of $(1/3)\ln(C\bar{N}_t)$, with $C = C_{A,t}$ or $C_{T,t}$, the experimental data are shifted and become coincident with those of the growth rate (Figs. 5 and 6), thus allowing the density of nuclei to be determined. The solid symbols in the figures illustrate the procedure.

In order to proceed further with the analysis, it is important to discuss the effects of the thermodynamic melting temperature and the possible existence of regime transitions on the procedure described earlier. Since the temperature interval, where the experimental data of the half-crystallization time and growth rate is hardly the same, the prediction

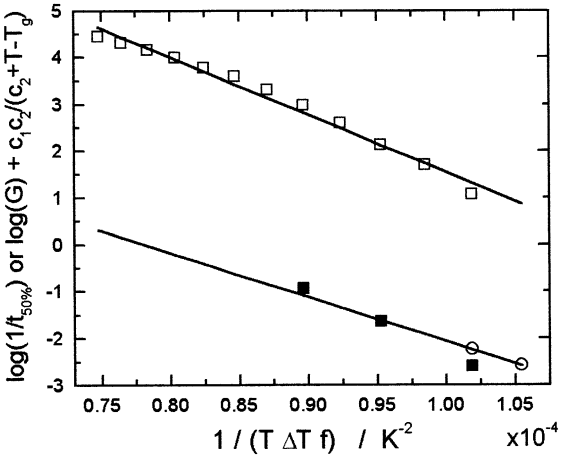

Fig. 6. Comparison of the values of the logarithm of the reciprocal of the half-crystallization time (□) with the values of the logarithm of the growth rate (○), for the isothermal crystallization of MDPE. The half-crystallization time plot, when subtracted of the contribution of the mean number of nuclei (first factor on the right-hand side of Eq. (7)) is shifted and becomes coincident with the growth plot (■). The experimental densities of nuclei are for 113, 115 and 117 °C. Time is in minutes and G in mm/min.

of the average density of nuclei in a broader temperature range indeed requires a discussion on regime transitions. In particular, the extrapolation of the values of K_g ($K_g^{1/t_{50\%}}$ or K_g^G) requires the same and constant regime in the temperature range where the experimental data are available and in the temperature region where the experimental data are being extrapolated to. However, when regime transitions do occur, they result in changes in slope of the $\ln(G)$ and $\ln(1/t_{50\%})$ plots. Within each regime, the average density of nuclei may then be calculated by a direct application of Eq. (8). For both materials studied in this work, a constant growth regime was assumed in the experimental temperature range. A discussion that supports this conclusion may be found in Appendix B.

4.3. Prediction of the density of nuclei from isothermal crystallization data

The results obtained for the density of nuclei are shown in Fig. 7(a) and (b) for POM and MDPE, respectively. Open triangles are the results predicted according to Eq. (13), from the half-crystallization time and growth rate data. Full triangles are for the results predicted from the kinetic constants and growth rate values, Eq. (14). Full circles are the experimental data. The prediction of the density of nuclei with the Tobin's approach, either for the results of $\ln(1/t_{50\%})$ (Eq. (13)) or for $\ln(k^{1/3})$ (Eq. (14)) follows more closely the experimental data. Similar results are shown in Fig. 7(b) for MDPE.

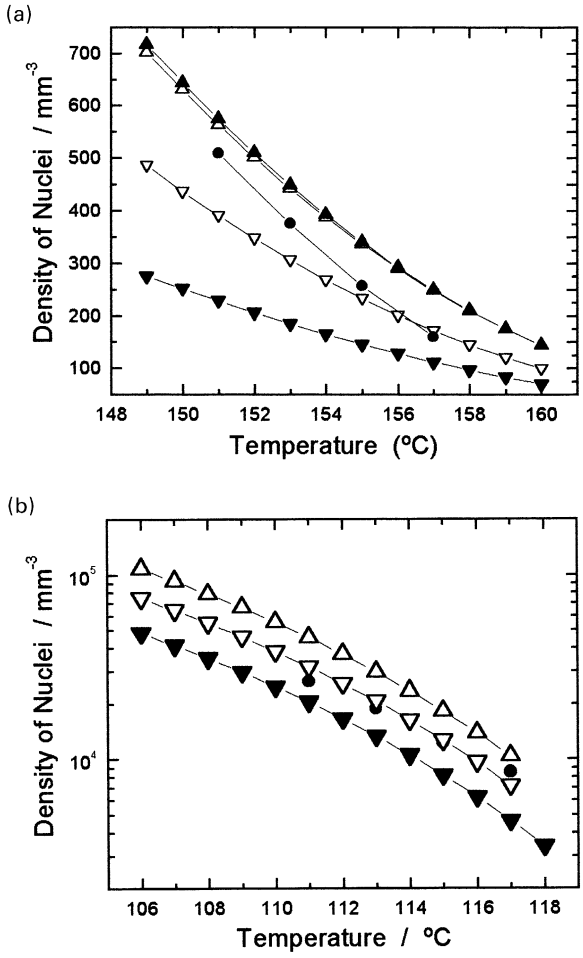

Fig. 7. Number of nuclei per unit volume determined from the results of DSC and optical microscopy with Eq. (13) (or Eq. (8)) using Avrami's (▽) and Tobin's (△) definitions for the half-crystallization time. The calculation of the density of nuclei from the kinetic constants and growth rates, Eq. (14) is shown, for Avrami, by (▼) and, for Tobin, by (▲). The experimental results determined for selected crystallization temperatures are also shown (●). (a) The results for POM and (b) the results for MDPE.

5. Discussion

An accurate application of the proposed method for the calculation of the mean number of nuclei requires an athermal (instantaneous) nucleation, with $n = 3$, which is not met in certain temperature ranges and for some materials. Also, as mentioned, the density of nuclei is greatly affected by the value of the thermodynamic melting temperature; in literature data, the dispersion of these values is large.

Concerning the experimental problems, an accurate temperature control, on both optical microscopy and DSC measurements, is of the utmost importance. In DSC isothermal crystallization experiments, at low temperatures, there is a temperature rise in the sample due to the sample's thermal resistance and to the release of the heat of crystallization. As a result, the average true sample temperature is higher than that the set isothermal crystallization temperature. The effect of the temperature rise in isothermal DSC scans is further discussed in other reports [33].

For the materials analysed in this work, it was found that the growth rate is constant, up to a large extent of the phase change, long after the impingement between spherulites, that the number of activated nuclei is almost constant since the start of the crystallization, and that the morphology is approximately spherical (with the exception of the upper and lower transcrystalline layers which, due to the relative large thickness of the samples used in the DSC experiments, have a minor role in the global phase change). It was also assumed that a second-stage crystallization process and eventual annealing of the crystals after crystallization play a minor role in the definition of the liquid to solid conversion half-time, which is the relevant quantity for all calculations carried out in this work. However, it must be stressed that neglecting the contribution of the nuclei in the columnar transcrystalline layers introduces another possibly small but nevertheless unquantifiable error.

Also, the detection of possible regime transitions is important, because the evaluation of the number of nuclei, by Eq. (13) or (14), is made by subtraction of K_g values. Very rarely, there is experimental data obtained by two techniques covering the same temperature range. As in the cases presented here, the growth rate data obtained by

optical microscopy must generally be extrapolated to lower temperatures.

Concerning again the experimental part of this work, we are dealing with overall crystallization kinetics, and the measured parameter which is used to record the process is the differential variation with time of the heat of crystallization released during the phase change. This is an average value for all samples (including portions with local heterogeneities). Further, experiments have been performed with other samples of the same material, having similar weights, in order to check for reproducibility. The check was performed and the reproducibility verified, which eliminates the role played by eventual heterogeneities on the overall crystallization kinetics. Different sections of the same sample, as well as sections of several samples, were used to measure the average number of nuclei at a particular crystallization temperature. So, the eventual role played by co-monomers was statistically evaluated and taken into account the measured data. In order to further check the validity of the procedure presented here, and to highlight its possible weaknesses, we decided to analyse independent literature data. A paper published by Chew et al. was selected [34]. They performed studies on the crystallization kinetics of a high-density polyethylene, with a thermodynamic melting temperature of 143 °C. According to the literature on regime transitions, a regime I–II should occur at 126 °C and a regime II–III at 120 °C. The temperature range studied by the authors is from 121 to 129 °C. The morphology obtained was round ringed spherulites at 121 °C, coarse non-ringed spherulites at 126 °C, and axialites at 127 °C (as expected in regime I).

The growth rate was measured at each crystallization temperature and the fraction of material transformed to solid phase, $X(t,T)$, was found at different times by "superimposing a square grid of points over the photograph and using a point-counting technique, whereby $X(t,T) = P_t/P_0$, where P_t is the number of points lying in the spherulites and P_0 the total number of points". From this, the time corresponding to 50% crystallization was calculated, a procedure that may only portray the behaviour of the entire three-dimensional sample after an adequate correction. This aspect is not entirely clear in Ref. [34].

Values of the *total number of spherulites* for each crystallization temperature are in Table 1 of Chew et al. [34]. For two particular temperatures, 121 and 128 °C, the number of spherulites, and the number of nuclei per unit area, were evaluated at different crystallization times and shown in figs. 6 and 7 of Ref. [34]. The number of spherulites was evaluated "by counting the number on the photographs and division by the area of the field of view". The *limiting number* was 1172 nuclei/mm^2 for 121 °C and 1182 nuclei/mm^2 for 128 °C. The *total number* referred in Table 1 of Ref. [34] is however much lower, 577 and 373, respectively, for the above two temperatures. Since the authors supplied no information, we assume that this *total number* refers to the entire sample at the end of crystallization. Since temperature gradients, albeit small, do exist in a microscopic slide, the information supplied by the authors for the half-crystallization time (as well as for the growth rate) may not be representative of the entire sample but only of the portion of the sample under direct observation.

Table 3
Values of the half-crystallization time and growth rate for HDPE. Values taken from Table 1 of Ref. [34]

T (°C)	$t_{50\%}$ (s)	G (nm/s)
121	30.5 ± 3.5	523 ± 135
128	25 000 ± 2500	1.55 ± 0.12

We will thus select the limiting number shown in figs. 6 and 7 of Ref. [34] and the corresponding values given by the authors for the growth rate and half-crystallization time. The latter are shown in Table 3.

The number of nuclei per unit area, supplied by the authors, is converted to number of nuclei per unit volume by using the Voronoi equation (15). From the growth rate and the half-crystallization time values, the number of nuclei is predicted using Eq. (13). The result is shown in Fig. 8. Of course, an athermal nucleation of spherulites is implicit in our calculations, which is acceptable for the temperature of 121 °C but not for 128 °C (as shown in fig. 8 of Ref. [34]). Use was also made of information on the error of measurement of the growth rates and half-crystallization times supplied by the authors. The dashed lines in Fig. 8 show the error effect on the prediction of the density of nuclei. The full symbols are the limiting values found by the authors for the above two temperatures. For the lower temperature (121 °C), the agreement is acceptable. The observed deviation at the higher temperature

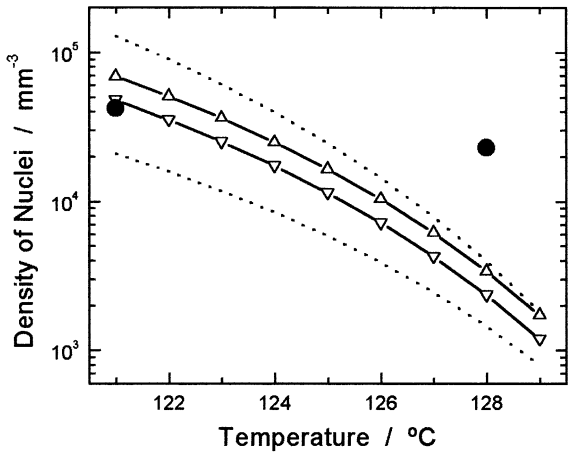

Fig. 8. Density of nuclei for HDPE calculated from data of Ref. [34]. Number of nuclei calculated using Avrami's (▽) and Tobin's (△) definitions for the half-crystallization time, from data of Table 1 of Ref. [34], with Eq. (13) (or Eq. (8)). The experimental results determined at 121 and 128 °C are also shown (●). Dotted lines represent the error in the calculation of the density of nuclei when use is made of error data on Table 1 of Ref. [34].

(128 °C) may be explained by the geometry of the structures grown in this temperature range and, eventually, by their type of nucleation.

6. Conclusion

A method was presented to evaluate and predict the density of nuclei from optical microscopy data and from information on the crystallization kinetics, either from the raw data, by using half-crystallization times, or by using the kinetic constants of the theoretical models. The method enables to predict the number of nuclei for crystallization temperatures below the experimental range, providing that a constant growth regime applies. Here, the method was only tested for isothermal experiments, but it is also extensible to non-isothermal experiments [27]. For a correct application of the method, the availability of experimental data in a wider temperature range is also desirable.

Appendix A

A possible procedure to be followed in the evaluation of the number of possible combinations of objects with different sizes (one made up of flexible, and the other of entirely rigid, identical chain segments, in different numbers), and in the evaluation of the corresponding entropy of mixing, is similar to the approach followed in the derivation of number of combinations between equal sized polymer chains and a solvent (or different polymer chains) used in the Flory–Huggins theory of polymer solutions (or mixtures). However, the procedure must be modified in order to restrict the placement of each embryo sub-unit (with the same size of a lattice base cell) in an immediate and spatially determined vicinity of the already assigned sub-units. This procedure must be followed for all embryos comprising the mixture and the number of possible combinations evaluated. Derivations so far made by the authors [35] amount to the estimation of the total number of available groups of x contiguous lattice cells satisfying a strictly defined spatial geometry to place a given number of nuclei (each made up of x segments). The number of embryos at equilibrium may then be evaluated following a procedure similar to the one followed by Kurz and Fisher, assuming an ideal mixture between embryos and segments. The details of this evaluation will be presented in another report [35], but the temperature dependence of the average number of nuclei obtained to form this evaluation is still approximately given by the Boltzmann factor of Eq. (9).

Appendix B

According to Hoffman [36] for POM, Delrin 150, a regime I–II transition occurs at $\Delta T = 27$ °C and a regime II–III at $\Delta T = 40$ °C. In his analysis, Hoffman used a value for the thermodynamic melting temperature found by Pelzbauer and Galeski [37], $T_m^0 = 471.5$ K = 198.3 °C. Our experimental calculation, based on Hoffman and Weeks extrapolation method, gave for POM, Delrin 150 °C, a $T_m^0 =$ 462.06 K = 188.91 °C in accordance with other literature data [30]. According to this analysis, in the temperature range studied by us we are in regime II, which may be confirmed by the values of the folding surface energies.

The slope of the curve of $[\ln(G) + C_1C_2/(C_2 + T - T_g)]$ in Fig. 5 is $K_g = 2.093 \times 10^5$ K^2. Assuming a $\Delta H_f^0 = 326 \pm$ 15 J/g and a density of the solid crystalline phase of 1.4185 g/cm^3 [28,29], we have $\Delta H_f^0 = 426.431$ J/cm^3. (Much lower values were used by Hoffman [36], 355 J/cm^3, and Plummer et al. [38], 380 J/cm^3, thus yielding higher values for the surface energies. We assume that in the conversion to J/cm^3 the density of the amorphous phase was used, $\rho_a \approx 1.1765$ g/cm^3). With the calculated values for ΔH_f^0 and T_m^0, and assuming that $b_0 = 4.471$ Å and $\sigma = 14.7$ mJ/m^2 (= 14.7 erg/cm^2), we have for regime II $\sigma_e = 219$ mJ/m^2 and for regime I and III, $\sigma_e =$ 109.5 mJ/m^2. Values for the folding surface energy referred in Hoffman's paper for regime II range between 183 and 205 mJ/m^2.

For MDPE, Fig. 6, with $T_m^0 = 143$ °C, the slope of the results of the growth rate is 0.945×10^5 K^2, consistent with the value found by Hoffman and Miller for regime II of polyethylenes of similar molecular weight [39]. According to Hoffman, a regime II–III should occur at a supercooling between 23 and 26 °C. Since no major changes in slope have been detected, it is assumed that regime II is maintained in the temperature range between 106 and 117 °C, and that regime II–III transition is shifted to lower temperatures. One of the possible causes for the change of regime II–III transition to lower temperatures is, according to Phillips and Lambert [40], the increase in the cross-linking or degree of branching. The value of the fold surface energy, calculated from our experimental data is coincident with those presented in the literature. With $T_m^0 = 143$ °C, $\sigma =$ 11.8 mJ/m^2, $b_0 = 4.15$ Å, $\Delta H_f^0 = 293$ J/g, (or $\Delta H_f^0 \approx$ 280 J/cm^3, with $\rho_c = 0.9556$ g/cm^3) we have $\sigma_e =$ 90.62 mJ/m^2 for $K_{g,II} = 0.955 \times 10^5$ K^2. With our value for K_g (0.945×10^5 K^2), the value obtained for σ_e is 89.63 mJ/m^2.

References

[1] Day M, Deslandes Y, Roovers J, Suprunchuk T. Polymer 1991;32:728.
[2] Deslandes Y, Sabir F-N, Roovers J. Polymer 1991;32:1267.
[3] Celli A, Zanotto ED. Thermochim Acta 1995;269/270:191.
[4] Kurz W, Fisher DJ. Fundamentals of solidification. Clausthal, Germany: Trans-Tech Publications, 1986.
[5] Turnbull D, Fisher JC. J Chem Phys 1949;17:71.
[6] Shultz J. Polymeric materials science. New York: Prentice-Hall, 1974.
[7] Gates DJ, Westcott M. Proc Roy Soc (Lond) 1988;A416:443.
[8] Gilbert EN. Ann Math Stat 1962;33:958.

[9] Miles RE. Suppl Adv Appl Probab 1972:243.
[10] Møller J. Adv Appl Prob 1989;21:37.
[11] Van de Weygaert R. Astron Astrophys 1994;283:361.
[12] Way JJ, Atkinson JR, Nutting J. J Mater Sci 1974;9:293.
[13] Friedrich K. Prog Colloid Polym Sci 1979;66:299.
[14] Avrami MJ. J Chem Phys 1941;9:177.
[15] Evans UR. Trans Faraday Soc 1945;41:365.
[16] Kolmogoroff AN. Izvest Akad Nauk SSR, Ser Math 1937;1:335.
[17] Tobin MC. J Polym Sci, Polym Phys Ed 1974;12:399.
[18] Wunderlich B. Macromolecular physics, vol. 2. New York: Academic Press, 1976.
[19] Eder G, Janeschitz-Kriegl H, Liedauer S. Prog Polym Sci 1990;15:629.
[20] Cruz Pinto JJC, Martins JA, Oliveira MJ. Colloid Polym Sci 1994;272:1.
[21] Hoffman JD, Davis GT, Lauritzen Jr JI. In: Hannay NB, editor. Treatise on solid state chemistry, vol. 3. New York: Plenum Press, 1976. p. 497.
[22] Porter DA, Easterling KE. Phase transformations in metals and alloys. UK: Van Nostrand Reinhold, 1987.
[23] Kittel C. Introduction to solid state physics. New York: Wiley, 1996.
[24] Johnson WA, Mehl RF. Trans Am Inst Miner Metal Engng 1939;135:416.
[25] Isayev AI, Cagtinani BF. Int Polym Process 2000;25:72.
[26] Schneider W, Köppl A, Berger J. Int Polym Process 1988;2:151.
[27] Eder G, Janeschitz-Kriegl H. Structure development during processing. 4: crystallization. In: Meijer HEH, editor. Materials science and technology, vol. 18. Weinheim: Verlag Chemie, 1994.
[28] Cramez MC, Martins JA, Oliveira MJ. Prediction of the average spherulite size in rotationally moulded parts. EPS 2000;241:139.
[29] Wunderlich B. Macromolecular physics, vol. 3. New York: Academic Press, 1980.
[30] Brandup J, Immergut EH, editors. Polymer handbook. 3rd ed. New York: Wiley/Interscience, 1989.
[31] Mark JE. Physical properties of polymers handbook. USA: American Institute of Physics, 1996.
[32] Martins JA, Cruz Pinto JJC. Polymer 2000;41:6875.
[33] Martins JA, Cruz Pinto JJC. Evaluation of the temperature rise in isothermal DSC scans. 12 ITAC, Copenhagen, 2000, p.172.
[34] Chew S, Griffiths JR, Stachurski ZK. Polymer 1989;30:874.
[35] Cruz Pinto JJC, Martins JA. Accurate calculation of the entropy of mixing of chain-like objects of different size and flexibility-relevance and consequences. In preparation.
[36] Hoffman JD. Polymer 1983;24:3.
[37] Pelzbauer Z, Galeski A. J Polym Sci, Part C 1972;38:23.
[38] Plummer CJG, Menu P, Cudré-Mauroux N, Kausch HH. J Appl Polym Sci 1995;55:489.
[39] Hoffman JD, Miller RL. Macromolecules 1988;21:3038.
[40] Phillips PJ, Lambert WS. Macromolecules 1990;23:2075.